



ELSEVIER

Journal of Magnetism and Magnetic Materials 248 (2002) 348–354



www.elsevier.com/locate/jmmm

Effect of A-site cation disorder on charge ordering and ferromagnetism of $\text{La}_{0.5}\text{Ca}_{0.5-y}\text{Ba}_y\text{MnO}_3$

V.N. Smolyaninova^{a,b,*}, S.E. Lofland^{a,c}, C. Hill^a, R.C. Budhani^{a,d},
Z. Serpil Gonen^e, B.W. Eichhorn^e, R.L. Greene^a

^aDepartment of Physics and Center for Superconductivity Research, University of Maryland, College Park, MD 20742, USA

^bNaval Research Laboratory, Washington, DC 20375, USA

^cDepartment of Chemistry and Physics, Center for Materials Research and Education, Rowan University, Glassboro, NJ 08028-1701, USA

^dDepartment of Physics, Indian Institute of Technology Kanpur, Kanpur-208016, India

^eDepartment of Chemistry, University of Maryland, College Park, MD 20742, USA

Received 29 January 2002

Abstract

The influence of an increase of average cation radius $\langle r_A \rangle$ and cation size disorder on transport and magnetic properties of half-filled $\text{La}_{0.5}\text{Ca}_{0.5-y}\text{Ba}_y\text{MnO}_3$ was studied. Despite an increase of $\langle r_A \rangle$, the ferromagnetism is inhibited in this compound due to the dominant effect of the cation size disorder. The charge-ordered antiferromagnetic state of this material was found to be stable to the influence of the cation size disorder.

© 2002 Elsevier Science B.V. All rights reserved.

PACS: 75.30.Vn; 71.30.+h; 75.50.Cc; 75.40.Cx

Keywords: Manganites; Charge ordering; Cation size disorder; Phase separation

1. Introduction

Determination of the electrical and magnetic ground states of the hole doped manganites with general formula $\text{R}_{1-x}\text{D}_x\text{MnO}_3$ (R is a rare earth and D is a divalent ion) has become an important topic of research in recent years [1–5]. Earlier, it

was recognized that the ground state of AMnO_3 depends solely on the average ionic radius $\langle r_A \rangle$ of the A-site ions [6]. Generally, for large $\langle r_A \rangle$, a charge delocalized ferromagnetic (FM) state is stable at low temperatures, whereas for small $\langle r_A \rangle$ the system goes to a charge-ordered (CO) antiferromagnetic (AFM) ground state, which is electrically insulating. A larger $\langle r_A \rangle$ enhances the bandwidth of the e_g electrons. This favors the ferromagnetic double exchange between Mn^{3+} and Mn^{4+} ions through the bridging oxygen. However, if the e_g bandwidth is narrow, as would be the case at the lower values of $\langle r_A \rangle$, the contribution to

*Corresponding author. Department of Physics and Center for Superconductivity Research, University of Maryland, College Park, MD 20742, USA. Fax: +202-767-1697.

E-mail address: smoly@anvil.nrl.navy.mil (V.N. Smolyaninova).

crystal bonding due to the kinetic energy of the delocalized e_g electron is not significant. The system gains much more energy by forming two interpenetrating Mn^{3+} and Mn^{4+} pseudocubic sublattices. Electron transfer between the sublattices is prohibited as it would destroy the CO state.

A transition from the CO to charge delocalized FM state has been realized by increasing the A-site ionic radius through substitution with divalent and trivalent ions of larger ionic radii. Manganites such as $(La_{1-x}Pr_x)_{0.7}Ca_{0.3}MnO_3$ and $Pr_{0.7}(Ca_{1-x}Sr_x)_{0.3}MnO_3$ are the best examples of systems whose ground state changes from CO to charge delocalized FM with increasing x [7]. Such substitutions also introduce local variations in the bond angles and bond lengths around the Mn^{3+} and Mn^{4+} ions. These deviations have been modeled by Rodriguez–Martinez and Atfield in terms of a parameter σ , which characterizes disorder, defined as the variance $\sigma^2 = \sum y_i r_i^2 - (\sum y_i r_i)^2 = \langle r_A^2 \rangle - \langle r_A \rangle^2$. Here y_i and r_i are fractional occupancy and the ionic radius of the i th cation, respectively [8]. For the case of a charge delocalized ferromagnet of given hole concentration, an increase of variance (σ^2) leads to a lower Curie temperature, a higher zero-temperature resistivity and a non-Curie–Weiss susceptibility at $T > T_C$ [8,9]. Maignan et al. have shown that for a fixed hole concentration and $\langle r_A \rangle$, an FM metal changes to a spin glass insulator at sufficiently large value of σ^2 [10]. The effect of the cation size disorder in the CO state has not been resolved yet. In Ref. [11], it was found that charge ordering is not affected by cation size disorder, while Ref. [12] reported the suppression of the CO for increased σ^2 values.

In this paper we report the effects of increase in $\langle r_A \rangle$ and σ^2 on transport and magnetic properties of the half-filled system $La_{0.5}Ca_{0.5}MnO_3$, which undergoes an FM to CO transition at $T \approx 140$ K. Both FM and CO phases are present in this compound at different temperatures, which gives an advantage for studying the influence of $\langle r_A \rangle$ and σ^2 on both of these phases simultaneously. We make substitution at the Ca sites ($\langle r_A \rangle = 1.18$ Å) with larger Ba ions ($\langle r_A \rangle = 1.47$ Å). A 24% site occupancy of Ba^{2+} increases $\langle r_A \rangle$ by 3.2%. The simple notion of a one-to-one correspondence

between the e_g bandwidth and $\langle r_A \rangle$ should have made the Ba-substituted $La_{0.5}Ca_{0.5}MnO_3$ a charge delocalized ferromagnet. On the contrary, we find that the materials approach the insulating state. We attribute this effect to a large increase in the variance with the Ba substitution.

2. Experimental details

Ceramic samples of $La_{0.5}Ca_{0.5-y}Ba_yMnO_3$ ($0 < y < 0.3$) were prepared by a standard solid-state-reaction technique. X-ray powder diffraction (XRD) patterns were recorded and analyzed using a Bruker D8 powder X-ray diffractometer and MDI software system, respectively. The specific heat was measured in the temperature range 2–20 K by relaxation calorimetry. The specific heat measurements have an absolute accuracy of $\pm 2\%$. The magnetization was measured with a commercial SQUID magnetometer in the magnetic field range 0–5.5 T and with a quantum design PPMS in fields up to 9 T. Resistivity was measured by a standard four-probe technique.

3. Results and discussion

The XRD patterns for the $La_{0.5}Ca_{0.5-y}Ba_yMnO_3$ samples with low Ba concentration ($y < 0.09$) show that samples are single phase with orthorhombic $Pbnm$ crystal symmetry. Lattice parameters obtained from the Rietveld analysis of the XRD data are given in Table 1. The unit cell volume is increasing systematically with the increase y , as expected for compounds with larger $\langle r_A \rangle$ (Table 1). However, for $y > 0.09$, a small amount of an impurity phase gives rise to additional reflections of low intensity in the XRD pattern. These additional reflections are due to the presence of hexagonal $BaMnO_3$ (space group $P6_3mc$). Similar phase separation was observed for the $La_{1-x}Ba_xMnO_3$ system for $x > 0.35$ [13]. While for $0.09 < y < 0.2$ concentrations the $BaMnO_3(110)$ and (103) reflections (highest intensities reflections) are just slightly above the background in the XRD pattern, the amount of the $BaMnO_3$ phase in $y = 0.3$ sample

Table 1

Variation of the lattice parameters, unit cell volume, $\langle r_A \rangle$, and σ^2 with Ba content y in $\text{La}_{0.5}\text{Ca}_{0.5-y}\text{Ba}_y\text{MnO}_3$

y	a (Å)	b (Å)	c (Å)	V (Å ³)	$\langle r_A \rangle$ (Å)	σ^2 (Å ²)
0	5.4302(2)	5.4210(2)	7.6418(2)	224.95(1)	1.198	0.00032
0.03	5.4327(4)	5.4191(3)	7.6367(4)	224.83(2)	1.207	0.00246
0.06	5.4410(2)	5.4270(2)	7.6373(2)	225.95(1)	1.215	0.00444
0.09	5.4525(2)	5.4329(2)	7.6446(2)	226.45512	1.224	0.00627
0.13	5.4634(2)	5.4416(2)	7.6522(3)	227.49(2)	1.236	0.00848
0.2	5.4810(2)	5.4597(2)	7.6864(2)	230.01(1)	1.256	0.01169

becomes more appreciable. At large values of σ^2 , the strain field associated with the local displacement of oxygen ions presumably becomes so large that the system undergoes a chemical phase separation. Therefore, we will not include the results on the $y = 0.3$ sample in subsequent discussion.

The temperature dependence of the resistivity of $\text{La}_{0.5}\text{Ca}_{0.5-y}\text{Ba}_y\text{MnO}_3$ ($0 < y < 0.2$) is shown in Fig. 1. Conductive and magnetic properties of the parent compound of this series, $\text{La}_{0.5}\text{Ca}_{0.5}\text{MnO}_3$, are extremely sensitive to the La to Ca ratio [14]. When the concentration of the Ca changes from 0.48 to 0.495, the low-temperature resistivity increases more than seven orders of magnitude. In this compositional range electronic phase separation occurs, and FM metallic and AFM charge-ordered phases coexist [14,15]. The resistivity of our $y = 0$ (no Ba) compound increases abruptly below $T = 120$ K due to the onset of the charge ordering, and has essentially no temperature dependence below 90 K (Fig. 1). There is a substantial hysteresis between cooling and warming around the CO transition. The rather low value of the resistivity at low temperature suggests the coexistence of metallic and CO phases. This temperature dependence of the resistivity correspond to the exact composition of $\text{La}_{0.51}\text{Ca}_{0.49}\text{MnO}_3$. We choose this particular starting composition because its low-temperature resistivity is several orders of magnitude higher than the resistivity of typical metallic manganite and several orders of magnitude lower than the resistivity of the completely CO compositions. This intermediate value of the resistivity is a good starting point for studying the effect of Ba doping on the Ca site.

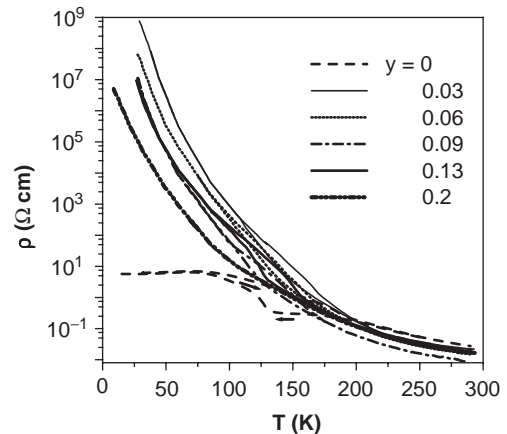


Fig. 1. Temperature dependence of the resistivity of $\text{La}_{0.5}\text{Ca}_{0.5-y}\text{Ba}_y\text{MnO}_3$ ($0 < y < 0.2$). Arrows denote the cooling and warming directions.

The temperature dependence of the resistivity $\rho(T)$ changes significantly when a small amount of Ba ($y = 0.03$) is introduced at the Ca site (Fig. 1). The $\rho(T)$ increases continuously as T decreases for the $y = 0.03$ (and also for $y = 0.06, 0.09, 0.13$, and 0.2) sample and has a low-temperature value many orders of magnitude higher than that of the parent $y = 0$ compound. The substitution of Ca by Ba increases of the average size of the A-site cation, $\langle r_A \rangle$ (Table 1) and brings the Mn–O–Mn bond angle closer to 180° . This leads to an increase of the transfer integral in the double exchange model. This should give rise to the FM metallic phase since the $\langle r_A \rangle$ values of our Ba doped samples are similar to the $\langle r_A \rangle$ values of typical FM metallic compositions of manganites. However, we observed the opposite tendency (Fig. 1). The probable explanation for this unexpected behavior is

disorder introduced by size mismatch of the A-site cations. The variance σ^2 , which is a measure of the disorder, changes abruptly from 0.00032 to 0.00246 Å² (Table 1) when Ba is introduced into the system. It has been shown previously that A-site cation disorder suppresses ferromagnetism in manganites: reduces the Curie temperature [9] and destroys a long-range FM ordering and metallic conduction [10]. In $\text{La}_{0.51}\text{Ca}_{0.49-y}\text{Ba}_y\text{MnO}_3$ A-site cation disorder destroys the metallic phase existing in the parent $y = 0$ compound. It seems that the A-site cation mismatch plays a more significant role than the increase of $\langle r_A \rangle$ (the bandwidth) in this compound.

The resistivity of $0.03 < y < 0.13$ samples exhibit a steep rise typical for a CO transition with hysteresis on cooling and warming in the vicinity of the CO transition. Apparently, A-site cation disorder does not destroy the charge ordering. If we define the onset of the steep rise of the resistivity as T_{CO} , we find that T_{CO} does not vary significantly for $0 < y < 0.13$ samples ($130 \text{ K} < T_{\text{CO}} < 150 \text{ K}$). No significant variation of T_{CO} with σ^2 was found in Ref. [11] for other half filled compositions with different σ^2 . However, Ref. [11] showed a strong decrease of T_{CO} with increase of $\langle r_A \rangle$, which we do not observe for $\text{La}_{0.5}\text{Ca}_{0.5-y}\text{Ba}_y\text{MnO}_3$. In case of $\text{La}_{0.5}\text{Ca}_{0.5-y}\text{Ba}_y\text{MnO}_3$, both $\langle r_A \rangle$ and σ^2 are increasing with y (Table 1). It appears that the charge delocalization induced by the increase of $\langle r_A \rangle$ (the bandwidth) is compensated by the localizing effect of A-site cation disorder.

The low-temperature specific heat of the $y = 0.09$ sample is shown in Fig. 2. The specific heat of this compound is larger than that of metallic $\text{La}_{0.625}\text{Ca}_{0.375}\text{MnO}_3$. The specific heat of an AFM insulator should be proportional to T^3 (a straight line through the origin, if plotted as C/T vs. T^2) since both lattice and an AFM spin-wave contributions have a T^3 temperature dependence. However, the specific heat of the $y = 0.09$ sample is not consistent with the specific heat of an AFM insulator, because it has an extra contribution, which manifests itself as the upward curvature in the C/T vs. T^2 plot. This extra contribution to the specific heat has been found before, but only in charge-ordered materials [16].

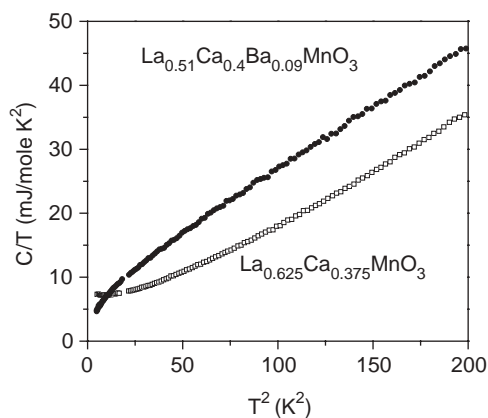


Fig. 2. Low temperature specific heat of $\text{La}_{0.51}\text{Ca}_{0.41}\text{Ba}_{0.09}\text{MnO}_3$ plotted as C/T vs. T^2 . Specific heat of $\text{La}_{0.625}\text{Ca}_{0.375}\text{MnO}_3$ is shown for comparison.

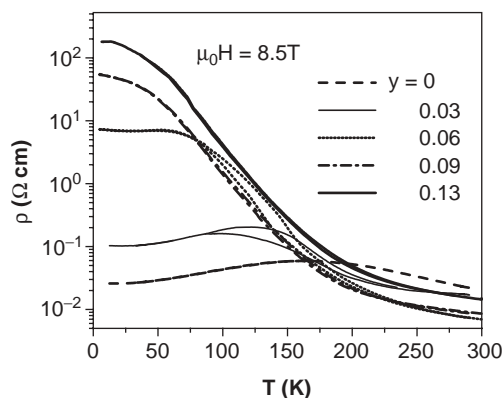


Fig. 3. Temperature dependence of the resistivity of $\text{La}_{0.5}\text{Ca}_{0.5-y}\text{Ba}_y\text{MnO}_3$ ($0 < y < 0.13$) in magnetic field 8.5 T on cooling and warming.

This is another indication that there is charge ordering in $\text{La}_{0.5}\text{Ca}_{0.5-y}\text{Ba}_y\text{MnO}_3$.

The temperature dependence of the resistivity of $0 < y < 0.13$ samples in a magnetic field of 8.5 T on cooling and warming is shown in Fig. 3. When the $y = 0$ sample is cooled in a magnetic field of 8.5 T, the CO state is destroyed completely, and the temperature dependence of the resistivity is typical of that found in FM metallic manganites. For all $0 < y < 0.13$ samples, the low-temperature value of resistivity after field cooling is reduced by many orders of magnitude, which corresponds to the “melting” of the CO state by the magnetic field.

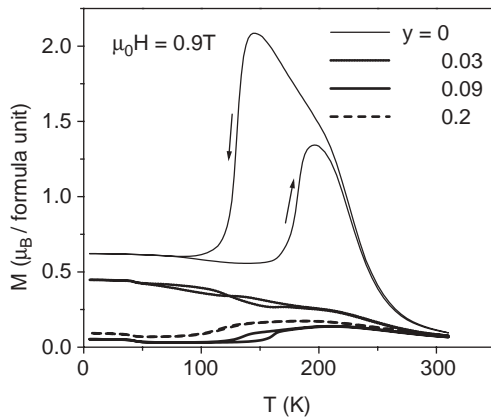


Fig. 4. Temperature dependence of magnetization of $\text{La}_{0.5}\text{Ca}_{0.5-y}\text{Ba}_y\text{MnO}_3$ ($0 < y < 0.2$) on cooling and warming in magnetic field of 0.9 T.

Substitution of Ca by Ba has a notable effect on the magnetic properties of $\text{La}_{0.5}\text{Ca}_{0.5-y}\text{Ba}_y\text{MnO}_3$. The temperature dependence of the magnetization of $0 < y < 0.2$ samples in a magnetic field of 0.9 T (just above the saturation field) on cooling and warming is shown in Fig. 4. On cooling, the $y = 0$ sample first undergoes a transition to the FM state (≈ 250 K), and then to a mostly AFM CO state (≈ 120 K). However, for Ba content as small as 0.03, ferromagnetism is strongly suppressed in this compound: the value of the magnetic moment of the $y = 0.03$ sample is more than 6 times smaller than for $y = 0$. Materials with larger Ba content have even smaller magnetization. This means that the localizing influence of A-site cation disorder is a more prominent factor than the increase in $\langle r_A \rangle$ (bandwidth) that would enhance the double-exchange mediated ferromagnetism. The low-temperature magnetization value is also suppressed with increase of Ba content (Fig. 4). Below ≈ 110 K the $y = 0$ sample is mostly AFM. However the low-temperature magnetization value of $y = 0$ sample is significant (18% of full spin alignment value), because both AFM and FM phases are present [15]. As at higher temperature, Ba doping suppresses the FM component, and much larger fraction of the sample is AFM ordered.

The magnetization of the samples after cooling in field of 9 T is shown in Fig. 5. The parent

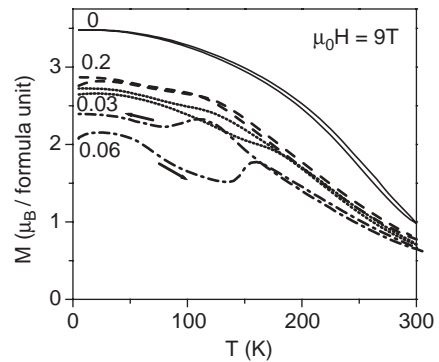


Fig. 5. Temperature dependence of magnetization of $\text{La}_{0.5}\text{Ca}_{0.5-y}\text{Ba}_y\text{MnO}_3$ ($0 < y < 0.2$) on cooling and warming in magnetic field of 9 T.

compound has a magnetization of $3.5 \mu_B$ /formula unit (full alignment), in accord with the metallic behavior found in electronic transport. For the other samples, in agreement with the resistivity data (Fig. 3), the AFM (CO) is not robust against field, although full alignment is not attained, i.e. some AFM remains. The magnetization of those samples also displays a thermal hysteresis between field-cooled cooling and field-cooled warming (not shown), presumably linked to CO and AFM.

The magnetic behavior is best understood from the M vs. H curves at low temperature. For $y = 0.03$ (Fig. 6a), there is saturation at ≈ 1 T at $0.35 \mu_B$ /formula unit in the zero-field cooled (ZFC) case. Above 5 T, a series of transitions take place, and one reaches about $1.5 \mu_B$ /formula unit by 9 T. This transition to the state with larger magnetic moment is an onset of the “melting” of the charge ordering which is accompanied by the transition to the FM state. As for other CO materials, cooling in the magnetic field of 9 T stabilizes the FM phase: the field-cooled (FC) curve, is representative of a simple FM. This behavior changes with increasing y . For $y = 0.09$ (Fig. 6b), application of 9 T to the zero-field cooled sample produces an FM component of $< 5\%$, and the magnetic field of 9 T is not sufficient to induce the transition to the FM state. The FC magnetization displays a wasp-waisted loop, which can be explained as the result of an FM component of about 60% coexisting with an AFM fraction which starts to be converted to the FM state in magnetic fields

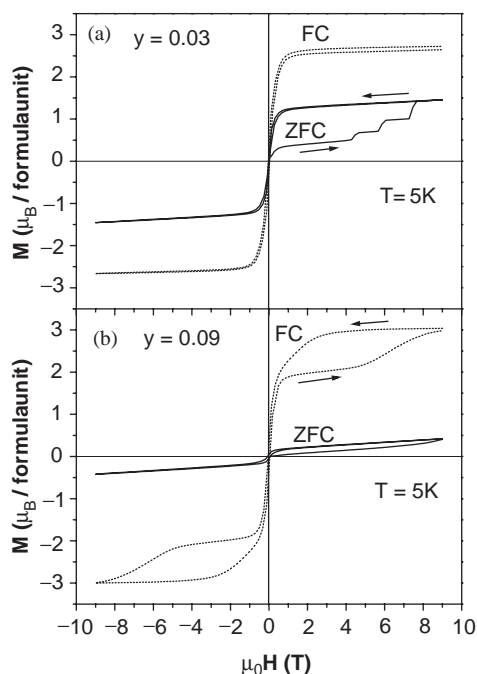


Fig. 6. Field dependence of magnetization of $\text{La}_{0.5}\text{Ca}_{0.5-y}\text{Ba}_y\text{MnO}_3$ at 5 K for (a) $y = 0.03$, (b) $y = 0.09$.

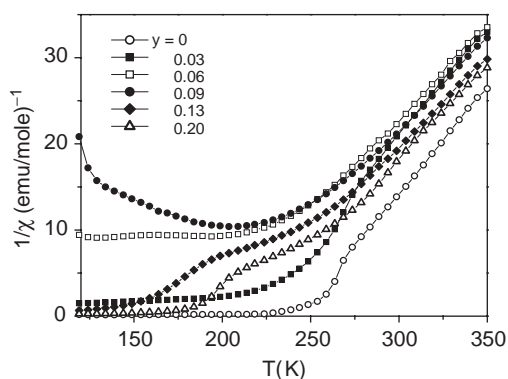


Fig. 7. Temperature dependence of the inverse susceptibility $\text{La}_{0.5}\text{Ca}_{0.5-y}\text{Ba}_y\text{MnO}_3$ ($0 < y < 0.2$).

above 5 T due to “melting” of the charge ordering in this magnetic field. This shows that for higher concentrations of Ba the AFM state (and accompanied CO state) becomes more stable to the influence of a magnetic field. Note that in no case does one observe spin glass behavior as seen by Maignan et al. [10].

The high-temperature susceptibility (Fig. 7) is also telling. While the low-temperature magnetization is rather disparate, the susceptibilities are remarkably similar, showing Curie-Weiss behavior above about 270 K. Furthermore the slopes are nearly identical and the extrapolated intercepts lie between 200 and 250 K, indicating that the effective moment remains constant and that there are only small modifications to the exchange. This is in contrast to the results of Ref. [9]. Here, it appears that the disorder is effective only at low temperature.

4. Conclusions

We have studied the influence of Ba content on transport and magnetic properties of the half-filled system $\text{La}_{0.5}\text{Ca}_{0.5-y}\text{Ba}_y\text{MnO}_3$ in which both $\langle r_A \rangle$ and σ^2 increase with Ba content. Despite a large increase of $\langle r_A \rangle$ and, consequently the bandwidth, substitution of Ca by Ba did not induce an FM metallic state. On the contrary, the FM ordering is suppressed in the FM state at higher temperatures ($150 \text{ K} < T < 250 \text{ K}$) and in the phase separated state at lower temperatures ($T < 150 \text{ K}$). We attribute these changes to the influence of the cation size disorder, which seems to play a more significant role than the increase of the bandwidth in this material. Our resistivity, magnetization and specific heat measurements indicate that the CO state is not affected significantly by the cation size disorder. Moreover, the insulating and AFM state of $\text{La}_{0.5}\text{Ca}_{0.5-y}\text{Ba}_y\text{MnO}_3$ become more stable to the influence of a magnetic field. Even for large values of σ^2 , the cation size disorder does not destroy the AFM ordering. It appears, that the localizing effect of the size mismatch disorder affects the double exchange mediated FM state more than the AFM state.

Acknowledgements

We thank Amlan Biswas for helpful discussions, Z. Li for the sample preparation, and R.M. Headley for the experimental help. This work is supported in part by the NSF-MRSEC at

Maryland, DMR #00-80008. SEL also acknowledges partial support by New Jersey Commission on Higher Education.

References

- [1] P. Schiffer, A.P. Ramirez, W. Bao, S.-W. Cheong, *Phys. Rev. Lett.* 75 (1995) 3336.
- [2] S. Mori, C.H. Chen, S.-W. Cheong, *Nature* 392 (1998) 473.
- [3] A. Moreo, S. Yunoki, E. Dagotto, *Science* 283 (1998) 2034.
- [4] J.M.D. Coey, M. Viret, S. Von Molnar, *Adv. Phys.* 48 (1999) 167.
- [5] Y. Tokura, N. Nagaosa, *Science* 288 (2000) 462.
- [6] H.Y. Hwang, S.-W. Cheong, P.G. Radaelli, M. Marezio, B. Batlogg, *Phys. Rev. Lett.* 75 (1995) 914; H.Y. Hwang, et al., *Phys. Rev. B* 52 (1995) 15 046; B. Raveau, et al., *J. Solid State Chem.* 117 (1995) 424.
- [7] K.H. Kim, M. Uehara, C. Hess, P.A. Sharma, S.-W. Cheong, *Phys. Rev. Lett.* 84 (2000) 2961.
- [8] L.M. Rodriguez-Martinez, J.P. Attfield, *Phys. Rev. B* 54 (1996) R15 622; L.M. Rodriguez-Martinez, J.P. Attfield, *Phys. Rev. B* 58 (1998) 2426.
- [9] J. Paul Attfield, *Chem. Mater.* 10 (1998) 3239.
- [10] A. Maignan, C. Martin, G. Van Tendeloo, M. Hervieu, B. Raveau, *Phys. Rev. B* 60 (1999) 15 214.
- [11] P.V. Vanitha, P.N. Santhosh, R.S. Singh, C.N.R. Rao, J.P. Attfield, *Phys. Rev. B* 59 (1999) 13539.
- [12] Y.Q. Wang, I. Maclaren, X.F. Duan, Z.H. Wang, B.G. Shen, *J. Appl. Phys.* 90 (2001) 488.
- [13] C. Roy, R.C. Budhani, *J. Appl. Phys.* 85 (1999) 3124.
- [14] K.H. Kim, M. Uehara, S.-W. Cheong, *Phys. Rev. B* 62 (2000) R11945.
- [15] Q. Huang, J.W. Lynn, R.W. Erwin, A. Santoro, D.C. Dender, V.N. Smolyaninova, K. Ghosh, R.L. Greene, *Phys. Rev. B* 61 (2000) 8895.
- [16] V.N. Smolyaninova, K. Ghosh, R.L. Greene, *Phys. Rev. B* 58 (1998) R14725; V.N. Smolyaninova, A. Biswas, X. Zhang, K.H. Kim, B.-G. Kim, S.-W. Cheong, R.L. Greene, *Phys. Rev. B* 62 (2000) R6093.